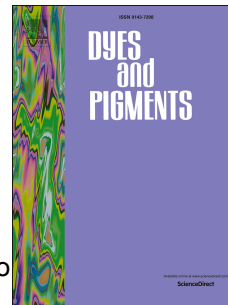


# Accepted Manuscript

Influence of the additional electron-withdrawing unit in  $\beta$ -functionalized porphyrin sensitizers on the photovoltaic performance of dye-sensitized solar cells

Futai Lu, Yaqing Feng, Xuexiang Wang, Yanming Zhao, Guang Yang, Jie Zhang, Bao Zhang, Zhixin Zhao



PII: S0143-7208(16)30996-2

DOI: [10.1016/j.dyepig.2016.12.027](https://doi.org/10.1016/j.dyepig.2016.12.027)

Reference: DYPI 5652

To appear in: *Dyes and Pigments*

Received Date: 20 October 2016

Revised Date: 24 November 2016

Accepted Date: 4 December 2016

Please cite this article as: Lu F, Feng Y, Wang X, Zhao Y, Yang G, Zhang J, Zhang B, Zhao Z, Influence of the additional electron-withdrawing unit in  $\beta$ -functionalized porphyrin sensitizers on the photovoltaic performance of dye-sensitized solar cells, *Dyes and Pigments* (2017), doi: 10.1016/j.dyepig.2016.12.027.

This is a PDF file of an unedited manuscript that has been accepted for publication. As a service to our customers we are providing this early version of the manuscript. The manuscript will undergo copyediting, typesetting, and review of the resulting proof before it is published in its final form. Please note that during the production process errors may be discovered which could affect the content, and all legal disclaimers that apply to the journal pertain.

Influence of the additional electron-withdrawing unit in  
 $\beta$ -functionalized porphyrin sensitizers on the photovoltaic  
performance of dye-sensitized solar cells

Futai Lu<sup>a,b,1</sup>, Yaqing Feng<sup>a,b,c,2</sup>, Xuexiang Wang<sup>d,3</sup>, Yanming Zhao<sup>b,4</sup>, Guang Yang<sup>b,5</sup>, Jie Zhang<sup>b,6</sup>, Bao Zhang<sup>a,c,7,\*</sup> and Zhixin Zhao<sup>e,8,\*</sup>

<sup>a</sup> School of Chemical Engineering and Technology, Tianjin University

Tianjin 300350, P. R. China

Tel.: +86-022-27892323. Fax: +86-022-27892323

<sup>b</sup> Tianjin Co-Innovation Center of Chemical Science and Engineering, Tianjin University,

Tianjin 300072, P. R. China

<sup>c</sup> Tianjin Engineering Research Center of Functional Fine Chemicals

<sup>d</sup> Department of Application of Chemical Engineering, Lanzhou Petrochemical College of

Vocational Technology, Lanzhou 730060, P. R. China

<sup>e</sup> Michael Grätzel Center for Mesoscopic Solar Cells, Wuhan National Laboratory for

ptoelectronics Department, School of Optical and Electronic Information, Huazhong

University of Science and Technology, 1037 Luoyu Road, Wuhan 430074, P. R. China

<sup>1</sup>lufutaitiger@126.com, <sup>2</sup>yqfeng@tju.edu.cn, <sup>3</sup>23205903@qq.com <sup>4</sup>zym84699384@163.com,

<sup>5</sup>176879931@qq.com, <sup>6</sup>zhjie@tju.edu.cn, <sup>7</sup>[baozhang@tju.edu.cn](mailto:baozhang@tju.edu.cn)\*, <sup>8</sup>zhixin-zhao@hust.edu.cn\*

\* Corresponding authors: [baozhang@tju.edu.cn](mailto:baozhang@tju.edu.cn)

## Abstract

The  $\beta$ -functionalized porphyrin containing an additional electron-withdrawing unit, 2,3-diphenylquinoxaline(DPQ) for **LP-5** or 2,1,3-benzothiadiazole (**BTD**) for **LP-6** with different electron-withdrawing abilities, between the porphyrin core and the anchoring group and the reference porphyrin dye (**LP-4**) have been designed and synthesized for DSCs. The influence of the additional electron-withdrawing units on molecular properties as well as photovoltaic performance of the corresponding DSCs was investigated systematically. Compared with **LP-4**, the introduction of additional electron-deficient unit at the porphyrin  $\beta$   $\pi$ -linker in **LP-5** and **LP-6** decreases the lowest unoccupied molecular orbital (LUMO) energy levels, resulting in the broader absorption spectra and significantly improved IPCE spectra in the region 350-500 nm, which ensures the better light-harvesting properties and the higher short-circuit current density ( $J_{sc}$ ). On the other hand, the introduction of additional acceptors of **LP-5** and **LP-6** induces dye aggregation and reduces the lifetime of the charge-separated states, which decreases the open-circuit voltage ( $V_{oc}$ ). Interestingly, the loss in  $V_{oc}$  is overcompensated by the improvement in  $J_{sc}$ . The study provides not only an alternative approach to design novel porphyrin sensitizers, but also an insight into how to manipulate the LUMO energy levels of porphyrin sensitizers via the  $\beta$ -linker modifications for the optimal photovoltaic applications.

Keywords: porphyrin; electron-withdrawing unit; additional acceptors; dye-sensitized solar cells

## 1. Introduction

Dye-sensitized solar cells (DSCs) have attracted considerable attention because of their relatively high light-to-electricity conversion efficiencies, ease of fabrication and low production costs [1]. In recent years, significant efforts have been devoted to improve cell efficiencies [2]. Ruthenium complexes are typical sensitizers in DSCs that exhibit power conversion efficiency of more than 11% [3]. However, the scarcity, high cost and the problems with isomerization during the purification may hamper their widespread application. Inspired by the process of solar energy collection by photosynthetic cores of bacteria and plants, people have designed and synthesized numerous porphyrins as the light harvester for applications in DSCs [4]. The intrinsic advantages of porphyrin-based dyes are the large absorption coefficient of their Soret and Q-bands in the visible region, versatile modification at the meso and  $\beta$  position of their core and facile tuning of their optical, photophysical and electrochemical properties [5-7].

Typical meso disubstituted D- $\pi$ -A porphyrin sensitizers composed of an dialkylamine or diarylamine as the donor, and an ethynyl benzoic acid as the acceptor, have been extensively investigated [8-9]. Although the meso-functionalized porphyrins are featured by inspiring power conversion efficiency (PCE), multistep synthetic procedures and the corresponding low overall yield are still big challenges [10-12]. Tetraarylporphyrins are easily achievable by the direct condensation of pyrrole and an aryl aldehyde, which could be functionalized at the  $\beta$ -pyrrolic position by relatively few synthetic steps [13-14]. However, few studies focused on the

$\beta$ -functionalized porphyrin sensitizers due to the relatively lower PCEs of the corresponding DSCs, compared to meso-substituted ones. In general, the modification of meso-tetraphenylporphyrins is mostly focused on the  $\beta$  linkage between the porphyrin core and the anchoring group as it serves primarily to extend  $\pi$  conjugation, leading to the enhancement of the molecule's light harvesting properties. So far, ethynyl benzene [10], dithienylethylene [11], ethane [15], pentadiene [15], ethenyl benzene [16] etc, have been successfully utilized as the  $\pi$  linkers. However, their role in light harvesting is limited. The best performance of  $\beta$ -functionalized zinc porphyrin **ZnBD<sub>2</sub>** was reported by Kim and co-workers, which contains a bis(4-tert-butylphenyl)amino group at the meso position and two 2,4-pentadienoic acid anchoring groups at the  $\beta$ -pyrrolic positions [16]. This porphyrin dye reaches a PCE of 8.2%, which is comparable to the performance of a **N<sub>3</sub>** dye (PCE = 7.7%) under the same condition.

Recently, a new type of organic dye with an additional electron-withdrawing unit introduced into the  $\pi$  bridge as an internal acceptor has been reported and characterized as a D-A- $\pi$ -A architecture, which is believed to optimize the molecule's optoelectronic properties via decreasing the lowest unoccupied molecular orbital (LUMO) energy levels, resulting in extension of the light absorption spectra and the improvement of the photovoltaic performance for use in DSCs [17-19]. Inspired by the success of the D-A- $\pi$ -A featured organic dyes, the electron-deficient units were also introduced to the porphyrin framework [20-25], resulting in the D-A- $\pi$ -A type porphyrin dye **SM315** which is reported to reach a PCE record of 13% for use in

porphyrin-sensitized solar cells (PSCs) without the requirement of a co-sensitizer [20]. The porphyrin dye **SM315** contains an additional electron-withdrawing **BTD** in the meso  $\pi$  linker (hereafter referred to as meso **BTD**-porphyrin). Therefore, a rational design of  $\pi$  linkers makes a great contribution to the development of PSCs. To the best of our knowledge, so far D-A- $\pi$ -A type porphyrin sensitizers with the electron-deficient **BTD** moiety are all modified at the meso position, and no studies on the influence of the introduction of an additional electron-withdrawing unit at the porphyrin  $\beta$  position on the performance of the resultant PSCs have reported.

Taking these points into account, we have designed and synthesized three porphyrin dyes **LP-4**, **LP-5** and **LP-6** which were functionalized at the  $\beta$ -pyrrolic position of 5,10,15,20-tetraphenylporphyrin. Based on the reference porphyrin dye **LP-4** which is featured with a typical D- $\pi$ -A configuration containing the ethynyl benzoic acid as the acceptor moiety, two electron-deficient groups with different electron-withdrawing abilities, 2,3-diphenylquinoxaline (**DPQ**) for **LP-5** and **BTD** for **LP-6** were introduced into the  $\pi$ -linker between the anchoring group and the porphyrin core. The influence of introducing different auxiliary acceptor on the porphyrins' optical and electrochemical properties and photovoltaic performance of PSCs based on these porphyrins are systematically investigated. The study would shed some light on how to manipulate the LUMO energy levels of porphyrin sensitizers via the modification of the  $\beta$ -linker for the optimal photovoltaic applications.

**Fig. 1** Molecular structure of the three porphyrin sensitizers**Scheme 1.** Synthetic route for three porphyrin sensitizers

## 2. Experimental

**Materials and characterization.** The synthetic routes for **LP-4**, **LP-5** and **LP-6** are shown in the Scheme 1. All reactions dealing with air- or moisture-sensitive compounds were carried out using standard Schlenk techniques. 5,8-Dibromo-2,3-diphenylquinoxaline (**3**) and  $\beta$ -Bromo-5,10,15,20-tetraphenylporphyrinato] zinc( $\square$ ) (**5**) were synthesized according to the literature methods [26, 27].

$^1\text{H}$  NMR spectra were recorded on a Bruker AV400 MHz spectrometer in  $\text{CDCl}_3$  or THF- $d_8$  with tetramethylsilane as a reference. MALDI-TOF-MS was obtained with a Bruker Autoflex ToF/ToF III instrument. The UV-Vis spectra of dyes in THF solution ( $3 \times 10^{-6}$  M) were measured using Shimadzu UV-1800 in 10 mm quartz cell Spectrometer. Cyclic voltammetry (CV) measurements were carried out with a Chenhua CHI600E electrochemical analyzer at a scan rate of 50 mV/s at room temperature: a glassy carbon electrode, a Pt electrode and an  $\text{Ag}/\text{Ag}^+$  electrode were used as the working electrode, counter electrode and reference electrode respectively;  $\text{Fc}/\text{Fc}^+$  (ferrocene/ferrocenium) redox couple was employed for calibration, and 0.1 M

tetrabutylammonium perchlorate (TBAP) in anhydrous THF for the supporting electrolyte.

**Fabrication and photovoltaic measurements of DSCs.** The photoanode was prepared by coating commercial nanocrystalline TiO<sub>2</sub> (P25) layer with the working area of 0.159 cm<sup>2</sup> and the thickness of 16 μm on the FTO conducting glass using screen-printing method followed by calcinations at 500 °C for 30 min. After immersed into a 40 mM aqueous TiCl<sub>4</sub> solution at 70 °C for 30 min and washed with water and ethanol, the films were heated again at 500 °C followed by cooling to the room temperature and soaked in a porphyrin dye solution (0.3 mM) with EtOH/toluene=1:1 at 25 °C for 3 h for dye loading onto the TiO<sub>2</sub> film. The redox electrolyte consists of 0.6 M 1-propyl-2,3-dimethylimidazolium iodide, 0.05 M I<sub>2</sub>, 0.1 M LiI and 0.5 M tert-butylpyridine in a mixture of acetonitrile and valeronitrile (volume ratio 85:15). The porphyrin dye-sensitized TiO<sub>2</sub> electrode, electrolyte and Pt foil as the counter electrode (purchased) were fabricated into a typical sandwich-structured cell. Details on cell fabrication can be found in our previous publications [28].

The photocurrent density-voltage (*J-V*) characteristics for PSCs were recorded on Keithley 2400 Source meter (solar AAA simulator, oriel China, calibrated with a standard crystalline silicon solar) under simulated AM 1.5 irradiation (100 mW cm<sup>-2</sup>). The irradiated area of the cell was 0.159 cm<sup>2</sup>, the active area of the cell is so small that no mask can be employed during the measurement. Monochromatic incident photon-to current conversion efficiency (IPCE) for the solar cells was performed on a

commercial setup (Q Test Station 2000 IPCE Measurement System, CROWNTECH, USA). Electrochemical impedance spectra (EIS) were scanned in a frequency range of 0.1-106 Hz and at an AC amplitude of 10 mV at room temperature with a Chenhua CHI600E analyzer.

### Synthesis of porphyrin sensitizers.

Compound **2**: 4-(methoxycarbonyl)phenylboronic acid (121 mg, 0.673 mmol, 1.2 equiv), 4,7-bromo-2,1,3-benzothiadiazole (**1**) (165 mg, 0.561 mmol), Pd(PPh<sub>3</sub>)<sub>4</sub> (65 mg, 0.056 mmol, 10 mol%), Na<sub>2</sub>CO<sub>3</sub> (71 mg, 0.673 mmol, 5 mol%) toluene (5 mL) and H<sub>2</sub>O (1 mL) were stirred at 90 °C for 12 hour, upon which no more starting material was detected by TLC. The mixture was poured into H<sub>2</sub>O and then extracted with CH<sub>2</sub>Cl<sub>2</sub>. The organic layer was dried over anhydrous MgSO<sub>4</sub> and the solvent was removed under reduced pressure. the residues were subjected to column chromatography using DCM/PE = 1/1 as eluent to afford the desired product **2** as a pale yellow solid (53 mg, yield 27%). <sup>1</sup>H NMR (400 MHz, CDCl<sub>3</sub>) δ 8.19 (d, *J* = 8.5 Hz, 2H), 7.98 (d, *J* = 8.5 Hz, 2H), 7.95 (d, *J* = 7.6 Hz, 1H), 7.63 (d, *J* = 7.6 Hz, 1H), 3.97 (s, 3H); <sup>13</sup>C NMR (100 MHz CDCl<sub>3</sub>): δ 166.7, 153.9, 152.8, 140.9, 132.8, 132.2, 129.9, 129.1, 128.7, 127.2, 114.2, 52.3.

Compound **4**: A mixture of 5,8-dibromo-2,3-diphenylquinoxaline (**3**) (330 mg, 0.69 mmol), 4-(methoxycarbonyl)phenylboronic acid (130 mg, 0.71 mmol) and tetrakis(triphenylphosphine) palladium(0) (12 mg, 0.01 mmol) was dissolved in 10 ml THF and sodium bicarbonate (75 mg, 0.71 mmol) in 1 mL water was added. After

stirring at 70 °C for 4 h under argon, the mixture was poured into water and extracted with CH<sub>2</sub>Cl<sub>2</sub>. The organic layers were separated, dried over magnesium sulfate and filtered. After evaporation of solvent, the residues were subjected to column chromatography using DCM/PE = 2/1 as eluent, Recrystallization from PE/DCM to give **4** as a yellow solid (172 mg, yield 35%). <sup>1</sup>H NMR (400 MHz, CDCl<sub>3</sub>) δ 8.20 (d, *J* = 8.4 Hz, 2H), 8.13 (d, *J* = 7.9 Hz, 1H), 7.88 (d, *J* = 8.4 Hz, 2H), 7.76–7.72 (m, 2H), 7.69 (d, *J* = 7.9 Hz, 1H), 7.56 (d, *J* = 6.9 Hz, 2H), 7.48–7.29 (m, 6H), 4.00 (s, 3H); <sup>13</sup>C NMR (101 MHz, CDCl<sub>3</sub>) δ 167.08, 153.11, 152.87, 142.20, 139.08, 139.04, 138.65, 138.41, 138.32, 132.90, 130.80, 130.28, 130.21, 130.05, 129.40, 129.33, 129.24, 128.36, 128.27, 124.13, 52.20.

Compound **6**: A mixture of the zinc complex of **5** (1 g, 1.32 mmol), triisopropylacetylene (0.61 mL, 3.33 mmol), Pd(PPh<sub>3</sub>)<sub>2</sub>Cl<sub>2</sub> (180 mg, 0.26mmol), CuI (76.6 mg, 0.39 mmol), THF (50 mL) and NEt<sub>3</sub> (6 mL) was gently refluxed for 4 h under dinitrogen. The solvent was removed under vacuum. The residue was purified by column chromatography (silica gel) using DCM/PE = 1/1 to as eluent to give the product **6** (926 mg, 82%) as a purple solid. <sup>1</sup>H NMR (400 MHz, CDCl<sub>3</sub>) δ 9.22 (s, 1H), 8.97 (d, *J* = 5.3 Hz, 4H), 8.89 (d, *J* = 4.7 Hz, 1H), 8.76 (d, *J* = 4.7 Hz, 1H), 8.27–8.19 (m, 6H), 8.16 (d, *J* = 7.0 Hz, 2H), 7.85–7.71 (m, 10H), 7.67 (t, *J* = 7.4 Hz, 2H), 1.05–1.22 (m, 21H). MALDI-TOF-MS: *m/z* calcd for C<sub>55</sub>H<sub>48</sub>N<sub>4</sub>SiZn, 856.29; found, 856.40 [M+].

Compound **7**: To a solution of porphyrin **6** (143 mg, 0.167 mmol) in dry THF (20 mL) was added TBAF (0.84 mL, 1M in THF). The solution was stirred at 23 °C for 30 min under dinitrogen. The mixture was quenched with H<sub>2</sub>O and then extracted with CH<sub>2</sub>Cl<sub>2</sub>. The organic layer was dried over anhydrous MgSO<sub>4</sub> and the solvent was removed under reduced pressure. The residue and methyl-4-iodobenzoate (218 mg, 0.835 mmol) were dissolved in a mixture of dry THF (36 mL) and NEt<sub>3</sub> (7 mL) and the solution was degassed with dinitrogen for 10 min; Pd<sub>2</sub>(dba)<sub>3</sub> (46 mg, 0.05 mmol) and AsPh<sub>3</sub> (102 mg, 0.33 mmol) were added to the mixture. The solution was refluxed for 4 h under dinitrogen. The solvent was removed under reduced pressure. The residue was purified by column chromatography (silica gel) using DCM/PE = 2/1 as eluent. Recrystallization from DCM/hexanes to give **7** (70 mg, yield 50%) as a purple solid. <sup>1</sup>H NMR (400 MHz, CDCl<sub>3</sub>) δ 9.25 (s, 1H), 8.92 (d, *J* = 7.0 Hz, 4H), 8.88 (d, *J* = 4.7 Hz, 1H), 8.78 (d, *J* = 4.7 Hz, 1H), 8.25–8.17 (m, 8H), 7.90 (d, *J* = 8.4 Hz, 2H), 7.82–7.71 (m, 9H), 7.66 (t, *J* = 7.3 Hz, 2H), 7.63–7.57 (m, 1H), 7.41 (d, *J* = 8.4 Hz, 2H), 3.86 (s, 3H). MALDI-TOF-MS: *m/z* calcd for C<sub>54</sub>H<sub>34</sub>N<sub>4</sub>O<sub>2</sub>Zn, 834.19; found, 834.27 [M<sup>+</sup>].

Porphyrin **LP-4**: Compound **7** (70 mg, 0.084 mmol) was dissolved in THF (30 mL), MeOH (20 mL) and a solution of NaOH (20 % w/w in water, 8 mL) added. The solution was heated at 40 °C for 2 hours upon which TLC (silica, DCM) indicated complete hydrolysis of the ester. The reaction mixture was diluted with DCM (100 mL) washed with water (100 mL), HCl (1M, 120 mL), water (100 mL), the organics dried (Na<sub>2</sub>SO<sub>4</sub>) and evaporated. The residue was loaded onto a short column (silica,

DCM then 1:9 MeOH/DCM) to afford a brown solid which was further purified by recrystallization (THF/MeOH) to afford the final product **LP-4** as a purple solid (51 mg, yield 75%).  $^1\text{H}$  NMR (400 MHz, DMSO)  $\delta$  9.03 (s, 1H), 8.76 (m, 4H), 8.72 (d,  $J$  = 4.7 Hz, 1H), 8.60 (d,  $J$  = 4.7 Hz, 1H), 8.23-8.12 (m, 9H), 7.96 (d,  $J$  = 8.4 Hz, 2H), 7.85–7.77 (m, 11H), 7.75–7.70 (m, 4H), 7.48 (d,  $J$  = 8.4 Hz, 2H). MALDI-TOF-MS:  $m/z$  calcd for  $\text{C}_{53}\text{H}_{32}\text{N}_4\text{O}_2\text{Zn}$ , 820.18; found, 820.24[M+].

Compound **8**: A mixture of porphyrin **6** (143 mg, 0.167 mmol), dry THF (20 mL) and TBAF (0.84 mL, 1M in THF) under the argon atmosphere was stirred at 23 °C for 30 min.  $\text{H}_2\text{O}$  was added and the resulting solution was extracted with  $\text{CH}_2\text{Cl}_2$ . The organic layer was dried ( $\text{MgSO}_4$ ) and the concentrated under reduced pressure. The residue and **4** (412 mg, 0.835 mmol) were dissolved in a mixture of dry THF (36 mL) and  $\text{NEt}_3$  (7 mL) and the solution was degassed with dinitrogen for 10 min;  $\text{Pd}_2(\text{dba})_3$  (46 mg, 0.05 mmol) and  $\text{AsPh}_3$  (102 mg, 0.33 mmol) were added to the mixture. The solution was refluxed for 4 h under dinitrogen. The solvent was removed under reduced pressure. The residue was purified by column chromatography (silica gel) using  $\text{DCM/PE} = 2/1$  as eluent. Recrystallization from  $\text{DCM/hexanes}$  to give **8** (89 mg, yield 48%) as a purple solid.  $^1\text{H}$  NMR (400 MHz,  $\text{CDCl}_3$ )  $\delta$  9.49 (s, 1H), 8.95 (d,  $J$  = 6.9 Hz, 4H), 8.90 (d,  $J$  = 4.7 Hz, 1H), 8.80 (d,  $J$  = 4.7 Hz, 1H), 8.31 (m, 4H), 8.27–8.18 (m, 4H), 8.04 (d,  $J$  = 8.3 Hz, 2H), 7.94 (d,  $J$  = 8.3 Hz, 2H), 7.91–7.72 (m, 12H), 7.73–7.65 (m, 4H), 7.62 (d,  $J$  = 6.6 Hz, 2H), 7.44–7.29 (m, 6H). MALDI-TOF-MS:  $m/z$  calcd for  $\text{C}_{74}\text{H}_{46}\text{N}_6\text{O}_2\text{Zn}$ , 1114.29; found, 1114.44 [M+].

Porphyrin **LP-5**: Compound **8** (89 mg, 0.08 mmol) was dissolved in THF (30 mL), MeOH (20 mL) and a solution of NaOH (20 % w/w in water, 8 mL) was added. The solution was heated at 40°C for 2 hours upon which TLC (silica, DCM) indicated complete hydrolysis of the ester. The reaction mixture was diluted with DCM (100 mL) washed with water (100 mL), HCl (1 M, 120 mL), water (100 mL), the organics dried (Na<sub>2</sub>SO<sub>4</sub>) and evaporated. The residue was loaded onto a short column (silica, DCM then 1:9 MeOH/DCM) to afford a brown solid which was further purified by recrystallization (THF/MeOH) to afford the final product **LP-5** as purple solid (69 mg, yield 78%). <sup>1</sup>H NMR (400 MHz, THF) δ 9.30 (s, 1H), 8.78 (d, *J* = 9.2 Hz, 4H), 8.73 (d, *J* = 4.7 Hz, 1H), 8.65 (d, *J* = 4.6 Hz, 1H), 8.29–8.19 (m, 4H), 8.15 (dd, *J* = 5.6, 2.3 Hz, 6H), 7.98 (d, *J* = 8.2 Hz, 2H), 7.91 (d, *J* = 7.6 Hz, 1H), 7.85–7.66 (m, 12H), 7.65–7.56 (m, 5H), 7.37 (t, *J* = 7.4 Hz, 1H), 7.65–7.56 (m, 5H). MALDI-TOF-MS: *m/z* calcd for C<sub>73</sub>H<sub>44</sub>N<sub>6</sub>O<sub>2</sub>Zn, 1110.28; found, 1110.37 [M<sup>+</sup>].

Compound **9**: A solution of porphyrin **6** (143 mg, 0.167 mmol) in dry THF (20 mL) under an argon atmosphere was treated with TBAF (0.84 mL, 1M in THF), then the resulting solution was stirred at 23 °C. After half an hour, the mixture was quenched with H<sub>2</sub>O and then extracted with CH<sub>2</sub>Cl<sub>2</sub>. The organic layer was washed (water and brine), dried over anhydrous MgSO<sub>4</sub> and concentrated. The residue and **2** (290 mg, 0.835 mmol) were dissolved in a mixture of dry THF (36 mL) and NEt<sub>3</sub> (7 mL) and the solution was degassed with dinitrogen for 10 min; Pd<sub>2</sub>(dba)<sub>3</sub> (46 mg, 0.05 mmol) and AsPh<sub>3</sub> (102 mg, 0.33 mmol) were added to the mixture. The solution was refluxed for 4 h under dinitrogen. The solvent was removed under reduced pressure. The

residue was purified by column chromatography (silica gel) using DCM/PE = 2/1 as eluent. Recrystallization from DCM/hexanes to give **9** (73 mg, yield 45%) as a purple solid.  $^1\text{H}$  NMR (400 MHz,  $\text{CDCl}_3$ )  $\delta$  9.42 (s, 1H), 8.92 (d,  $J$  = 8.0 Hz, 4H), 8.88 (d,  $J$  = 4.7 Hz, 1H), 8.77 (d,  $J$  = 4.7 Hz, 1H), 8.31–8.17 (m, 8H), 8.14 (d,  $J$  = 8.4 Hz, 2H), 8.08 (d,  $J$  = 8.3 Hz, 2H), 7.76 (t,  $J$  = 7.5 Hz, 10H), 7.65–7.56 (m, 3H), 7.46 (t,  $J$  = 7.5 Hz, 1H), 3.91 (s, 3H). MALDI-TOF-MS:  $m/z$  calcd for  $\text{C}_{60}\text{H}_{36}\text{N}_6\text{O}_2\text{SZn}$ , 968.19; found 968.28 [M+].

Porphyrin **LP-5**: Compound **9** (73 mg, 0.076 mmol) was dissolved in THF (30 mL), MeOH (20 mL) and a solution of NaOH (20 % w/w in water, 8 mL) was added. The solution was heated at 40°C for 2 hours upon which TLC (silica, DCM) indicated complete hydrolysis of the ester. The reaction mixture was diluted with DCM (100 mL) washed with water (100 mL), HCl (1 M, 120 mL), water (100 mL), the organics dried ( $\text{Na}_2\text{SO}_4$ ) and evaporated. The residue was loaded onto a short column (silica, DCM then 1:9 MeOH/DCM) to afford a brown solid which was further purified by recrystallization ( $\text{Et}_2\text{O}/\text{MeOH}$ ) to afford the final product **LP-6** as a purple solid (59 mg, yield 81%).  $^1\text{H}$  NMR (400 MHz, THF)  $\delta$  9.26 (s, 1H), 8.82 (d,  $J$  = 7.3 Hz, 4H), 8.77 (d,  $J$  = 4.7 Hz, 1H), 8.68 (d,  $J$  = 4.7 Hz, 1H), 8.26–8.15 (m, 12H), 7.95 (d,  $J$  = 7.4 Hz, 1H), 7.81–7.70 (m, 9H), 7.69–7.60 (m, 3H), 7.55 (t,  $J$  = 7.5 Hz, 1H). MALDI-TOF-MS:  $m/z$  calcd for  $\text{C}_{59}\text{H}_{34}\text{N}_6\text{O}_2\text{SZn}$ , 954.17; found, 954.24 [M+].

### 3. Results and discussion

#### 3.1 Synthesis

The two key intermediate **2** and **4** were prepared by a Suzuki coupling reaction. In the next step, these electron-withdrawing unit were attached to the porphyrin core through a triple bond by a two-step Sonogashira coupling reaction. Finally, the Zn(II)-porphyrin sensitizers **LP-4**, **LP-5** and **LP-6** were obtained via hydrolysis. The dyes were obtained as a purple solid and soluble in most organic solvents, such as THF, DMF and DMSO.

#### 3.2 Photophysical properties

The UV-vis spectra of the metalloporphyrins **LP-4**, **LP-5** and **LP-6** in THF solvent are shown in Fig. 2a, and the corresponding absorption maxima and extinction coefficients for the Soret- and Q-bands are listed in Table 1. The absorption spectrum of **LP-4** displays three absorption peaks at 435 nm, 566 nm, and 603 nm, which are assigned as the  $\pi$ - $\pi^*$  transitions of the conjugated system and intramolecular charge transfer (ICT) transitions of the D- $\pi$ -A conjugated backbone [29]. The introduction of **DPQ** and **BDT** acceptor units had a significant impact on the absorption spectra of **LP-5** and **LP-6**, most evident by the splitting of the Soret band, resulting in a shoulder at 464 nm (for **LP-5**) and 471 nm (for **LP-6**) next to the maximum Soret band, respectively, but the absorption intensity are significantly decreased. Furthermore, the Q-bands of **LP-5** and **LP-6** were slightly red-shifted to 605 nm and 606 nm, respectively. It is believed that spectrum broadening and red-shift can be attributed to the increasing of the  $\pi$ -conjugation and the facilitated electron transfer from the

porphyrin to the acceptor (ICT) due to the introduction of additional electron-withdrawing acceptor. Both the splitting and red-shifting of the absorbance maxima for **LP-5** and **LP-6** were consistent with those previously reported meso **BTD**-porphyrin [20]. However, compared to **LP-5**, **LP-6** has similar absorption properties but the Soret band is more red-shifted, which suggests that the larger the electron withdrawing nature of the additional acceptor unit, the greater red-shift in the photoresponse, which is also consistent with the results obtained for the metal free organic dyes by Tian group [30]. Furthermore, there is a broadened absorption spectra of the porphyrin dyes absorbed on the TiO<sub>2</sub> film compared with the dyes in the solution especially for Soret band (Fig. 2b), indicating the formation of *J*-aggregates [31]. The fluorescent emission spectra of **LP-4**, **LP-5** and **LP-6** were obtained in THF solution, and the major emission bands observed at 616, 619 and 618 nm, respectively. The Stoke shifts for **LP-4**, **LP-5** and **LP-6** were 13 nm, 14 nm and 12 nm, respectively, which are smaller compared to metal-free organic dyes, suggesting a smaller energy required for geometrical reorganization of porphyrin dyes at photoexcited state [32-33].

**Fig. 2** UV-visible absorption spectra of compound **LP-4**, **LP-5** and **LP-6** (a) in THF solutions and (b) on transparent TiO<sub>2</sub> films (4  $\mu$ m).

**Table 1** Photophysical properties of the three sensitizers

### 3.3 Electrochemical properties

Cyclic voltammetric (CV) data for **LP-4**, **LP-5** and **LP-6** are shown in Table 2 and Fig. 3. The highest occupied molecular orbital (HOMO) energy levels are located at -5.15, -5.22 and -5.23 eV, respectively. These values are all more negative than the energy level of  $I/I_3^-$  redox (-4.9 eV) guaranteeing efficient dye regeneration [34]. It is shown that the HOMO energy levels of **LP-5** and **LP-6** were more negative than that of **LP-4**. Interestingly, these results are different from those of the meso **BTD**-porphyrin [20], in which the HOMO energy levels remain unchanged after introducing an additional electron withdrawing unit into the meso  $\pi$ -linker. The LUMO energy levels ( $E_{LUMO}$ ) of the three dyes were determined to be -3.08, -3.17 and -3.19 eV, respectively, which are significantly lower than the conduction band edge energy level of the  $TiO_2$  electrode (-3.9 eV), ensuring an efficient injection process from the excited state of the dyes into the  $TiO_2$  electrode [35]. Compared to **LP-4**, **LP-5** and **LP-6** containing **DPQ** and **BTD** units in the porphyrin frame show more negative LUMO levels and the decreased energy gap. Hence, the electronic transition from HOMO to LUMO orbitals in **LP-5** and **LP-6** was facilitated, which is consistent with an enhanced ICT character, and the red-shifting observed in the absorption spectrum of **LP-5** and **LP-6**. Furthermore, a comparison between the energy levels of **LP-5** and **LP-6** suggests that with the increasing of the electron-withdrawing capability of the additional auxiliary acceptor (**BTD**>**DPQ**), both the HOMO and LUMO levels and the LUMO-HOMO energy gap are decreased [36].

**Fig. 3** Energy levels (eV) of HOMO and LUMO molecular orbitals for the three sensitizers

**Table 2** Electrochemical data for the porphyrin sensitizers

### 3.4 Computational Analysis

We performed theoretical calculations based on density functional theory (DFT) at the B3LYP/6-31G level to investigate the frontier molecular orbitals and the geometrical structures of **LP-4**, **LP-5** and **LP-6**. As shown in Fig. 4, the HOMO of the three porphyrin dyes lies predominantly on the porphyrin core. Compared with that of **LP-4**, the LUMO of **LP-5** and **LP-6** shows a significant shift through the acceptor due to the presence of additional electron-withdrawing units (**DPQ** and **BTD**), and a more significant shift is observed for **LP-6** with a stronger electron-withdrawing **BTD** group. These results are consistent with those obtained in the experiment and could explain the greater charge transfer characteristics of **LP-5** and **LP-6**. Furthermore, in the optimized configurations, the dihedral angle between the porphyrin core and the neighboring benzene ring in **LP-4** is  $3^\circ$ , however, upon the introduction of additional electron-withdrawing units, the dihedral angles between the porphyrin core and the **DPQ** and **BTD** unit are  $23^\circ$  and  $6^\circ$ , respectively, and the dihedral angles between the **DPQ** and **BTD** unit and the neighboring benzene ring are  $45^\circ$  and  $37^\circ$ , respectively. Compared to **LP-6**, the more significant molecular twist of **LP-5** will decrease the effective conjugation length and weaken the charge transfer interaction, which explains the relatively blue-shifted absorption spectra of **LP-5**.

**Fig. 4** Calculated frontier molecular orbitals for the porphyrin dyes.

### 3.5 Photovoltaic performance of DSSCs

**LP-4**, **LP-5** and **LP-6** were used to fabricate solar cells using an iodine electrolyte and measured under illumination condition (AM 1.5G 100 mW cm<sup>-2</sup>). The photocurrent density-voltage (*J-V*) curves are shown in Fig. 5a and the corresponding detailed parameters are collected in Table 3. The short circuit current (*J*<sub>sc</sub>) of the PSCs fabricated with **LP-4** and **LP-5** was 7.60 mA cm<sup>-2</sup> and 9.03 mA cm<sup>-2</sup> with overall conversion efficiencies of 4.02% and 4.47%, respectively. The **LP-6** sensitized cell gave a *J*<sub>sc</sub> of 11.47 mA cm<sup>-2</sup>, *V*<sub>oc</sub> of 0.71 V, and FF of 0.74, corresponding to an overall conversion efficiency of 6.14%. The highest PCE of **LP-6** reached about 80% of the **N-719** based cell measured under the same condition. To clarify the influence of the introduction of an electron withdrawing unit into the β π-linker of the dyes on the device performances, we have measured the amount of dyes absorbed on TiO<sub>2</sub> (Table 3). As shown in Table 3, the dye loading results (1.41\*10<sup>-7</sup> mol cm<sup>-2</sup> for **LP-4**, 1.66\*10<sup>-7</sup> mol cm<sup>-2</sup> for **LP-5**, and 1.59\*10<sup>-7</sup> mol cm<sup>-2</sup> for **LP-6**) increased with the introduction of additional withdrawing units. Therefore, one reason for the enhanced *J*<sub>sc</sub> values for **LP-5** and **LP-6** could be their increased dye loading amounts. It is believed that another reason for the greater *J*<sub>sc</sub> achieved for **LP-5** and **LP-6** might be the enhanced intramolecular charge transfer and the broader absorption spectra due to the presence of electron-withdrawing units (**DPQ** and **BTD**) between the porphyrin core and anchoring group. Furthermore, the cathodic cyclic voltammetry test

suggested that the LUMO energy levels of **LP-5** and **LP-6** are more negative than the energy level of  $I/I_3^-$  redox when compared to that of **LP-4**, providing sufficient regeneration driving force. Overall, the introduction of the electron-withdrawing **BTD** leads to a  $J_{sc}$  value as high as  $11.47 \text{ mA cm}^{-2}$  for **LP-6**-based cell which is significantly greater than that of the cell sensitized by **LP-4**. However, compared with that of **LP-6** based cell, the  $J_{sc}$  value of **LP-5** cell dropped significantly, which is believed to be originated from the smaller electron-withdrawing nature of the additional acceptor.

It is also found the  $V_{oc}$  values achieved in **LP-4** and **LP-6**-based cells are greater than that of **LP-5** cell. The  $J$ - $V$  curves in dark as shown in Fig. 5a suggest that the dark current in PSCs based on **LP-4** and **LP-6** is smaller than that of **LP-5**, indicating that the increase in  $V_{oc}$  for **LP-4** and **LP-6**-based cells was achieved by suppressing the injected electron recombination rather than negative shift in CB of  $\text{TiO}_2$ .

The incident photo-to-current conversion efficiency (IPCE) spectra of **LP-4**, **LP-5** and **LP-6** were performed to further understand the correlation between the absorption and  $J_{sc}$  values (Fig. 5b). Compared to **LP-4**, it can be seen that both **LP-5** and **LP-6** with the additional electron-withdrawing unit have higher and extended absorption from 350 to 520 nm which is consistent with the splitted Soret band absorptions of **LP-5** and **LP-6** shown in Fig. 2a. Among three dyes, the IPCE value of **LP-6** is the highest and broadest, and over 50% IPCE from 350 to 650 nm achieved. The highest IPCE value and broadest absorption range of **LP-6** ensured the highest  $J_{sc}$

value and the best cell performance.

Electrochemical impedance spectroscopy (EIS) is a powerful technique of characterizing the important interfacial charge transfer and carrier transportation process in DSCs. The Nyquist plots (Fig. 6a) show the middle semicircle in the middle-frequency region, representing the resistance of charge transfer from  $\text{TiO}_2$  to the electrolyte. The larger middle semicircles for **LP-4** based DSCs mean that it is more difficult for charge transfer from  $\text{TiO}_2$  to the electrolyte for the device, which is consistent with the smaller dark current for **LP-4** dye observed in  $J$ - $V$  test. As we know, the photovoltage of a DSC is intrinsically influenced by the degree of electron recombination reaction [37-38]. Thus, the EIS Nyquist results are consistent with the  $V_{oc}$  values listed in Table 3. These results indicate that the introduction of electron-withdrawing units (**BTD** and **DPQ**) into the  $\pi$ -spacer of **LP-4** can facilitate the charge recombination, which result in the decrease the loss of the photovoltage of the device, which is consistent with results obtained from the BTD-meso porphyrin dye[20-21].

In the Bode phase plots (Fig. 6b), the frequency peak is indicative of the charge-transport process of injected electrons in  $\text{TiO}_2$ . The electron lifetime ( $\tau_e$ ) calculated through the equation  $\tau_e=1/(2\pi\omega_{max})$  ( $\omega_{max}$  is the maximum frequency in the Bode plot) can further explain the  $V_{oc}$  changes for **LP-4**, **LP-5** and **LP-6** -sensitized solar cells [39-40]. The  $\omega_{max}$  of the three dyes were found to be in the order **LP-4** < **LP-6** < **LP-5**, and thus the electron lifetime were to increase in the order

**LP-5** < **LP-6** < **LP-4**. Thus, the relatively highest  $V_{oc}$  of **LP-4** could be further explained. However, the loss of  $V_{oc}$  is overcompensated by a gain in  $J_{sc}$ , resulting in the superior performance of the **LP-5** and **LP-6** dyes.

**Fig. 5** (a) The J-V curves and (b) the IPCE profiles of LP-4, LP-5 and LP-6 sensitizers

**Fig. 6** Nyquist plots (a) and Bode-phase plots (b) of electrochemical impedance spectra measured at a forward bias of - 0.6 V under dark conditions for the DSSCs.

**Table 3** Photovoltaic parameters of porphyrin-sensitized solar cells

#### 4. Conclusions

In summary, two different electron-deficient units (**DPQ** for **LP-5** and **BTD** for **LP-6**) were first introduced into the  $\pi$ -linker at the  $\beta$ -pyrrolic position of 5,10,15,20-tetraphenylporphyrin. It was found that the introduction of auxiliary acceptor exhibits enhanced light-harvesting efficiency and relatively higher  $J_{sc}$  values. However, the DSCs based on **LP-5** and **LP-6** display shorter electron lifetime and facilitated charge recombination rate, resulting in a lower  $V_{oc}$  values compared to the reference dye **LP-4** without the additional electron-withdrawing unit. Interestingly, the decreased  $V_{oc}$  was overcompensated by a gain in  $J_{sc}$ , resulting in the superior performance, the optimized PCE of **LP-6** reached to 6.14% with a  $V_{oc}$  of 710 mV, a  $J_{sc}$  of 11.47 mA cm<sup>-2</sup> and a FF of 0.74. This finding provides an alternative way to

design and synthesize efficient and novel porphyrin sensitizers via the modification of porphyrin  $\beta$   $\pi$ -linkers for photovoltaic applications. Further studies on the molecular design for the photovoltaic devices with simultaneously improved  $J_{sc}$  and  $V_{oc}$  values are also in progress.

### Acknowledgement

This work was supported by National Natural Science Foundation of China (No. 21476162). The acknowledgment is also extended to China International Science and Technology Project (No. 2012DFG41980, S2016G3413).

### Reference

- [1] O'Regan B, Grätzel M. A low-cost, high-efficiency solar cell based on dye-sensitized colloidal TiO<sub>2</sub> films. *Nature* 1991; 353:737-40.
- [2] Grätzel M. Photoelectrochemical cells. *Nature* 2001; 414:338-44.
- [3] Chen CY, Wang MK, Li JY, Pootrakulchote N, Alibabaei L, Ngocle Ch, Decoppet JD, Tsai JH, Grätzel C, Wu CG, Zakeeruddin SM, Grätzel M. Highly efficient light-harvesting ruthenium sensitizer for thin-film dye-sensitized solar cells. *ACS Nano* 2009; 3: 3103-9.
- [4] Law CJ, Roszak AW, Southall J, Gardiner AT, Isaacs NW, Cogdell RJ. The structure and function of bacterial light-harvesting complexes. *Molecular Membrane Biology* 2004; 21:183-91.

- [5] Li LL, Diau EWG. Porphyrin-sensitized solar cells. *Chem Soc Rev* 2013; 42:291-304.
- [6] Urbani M, Grätzel M, Nazeeruddin MK, Torres T. Meso-substituted porphyrins for dye-sensitized solar cells. *Chem Rev* 2014, 114, 12330-12396.
- [7] Higashino T, Imahori H. Porphyrins as excellent dyes for dye-Sensitized solar cells: recent developments and insights. *Dalton Trans* 2015; 44:448-63.
- [8] Luo J, Xu M, Li R, Huang KW, Jiang C, Qi Q, Zeng W, Zhang J, Chi C, Wang P, Wu J. N-Annulated perylene as an efficient electron donor for porphyrin-based dyes: enhanced light-harvesting ability and high-efficiency Co(II/III)-based dye-sensitized solar cells. *J Am Chem Soc* 2014; 136:265-72.
- [9] Yella A, Lee H, Tsao H, Yi C, Chandiran A, Nazeeruddin M, Diau EG, Yeh C, Zakeeruddin SM, Grätzel M. Porphyrin-sensitized solar cells with cobalt (II/III)-based redox electrolyte exceed 12% efficiency. *Science* 2011; 334:629-34.
- [10] Ishida M, Hwang D, Koo YB, Sung J, Kim DY, Sessler JL, Kim D.  $\beta$ -(ethynylbenzoic acid)substituted push-pull porphyrins: DSSC dyes prepared by A direct palladium-catalyzed alkynylation reaction. *Chem Commun* 2013; 49:9164-6.
- [11] Carlo GD, Biroli AO, Tessore F, Pizzotti M, Mussini PR, Amat A, De Angelis F, Abbotto A, Trifiletti V, Ruffo R. Physicochemical investigation of the

- panchromatic effect on  $\beta$ -substituted  $\text{Zn}^{\text{II}}$  porphyrinates for DSSCs: the role of the  $\pi$  bridge between a dithienylethylene unit and the porphyrinic ring. *J Phys Chem C* 2014; 118:7307-20.
- [12] Di Carlo G, Caramori S, Trifiletti V, Giannuzzi R, De Marco L, Pizzotti M, Biroli AO, Tessore F, Argazzi R, Bignozzi CA. Influence of porphyrinic structure on electron transfer processes at the electrolyte/dye/ $\text{TiO}_2$  interface in PSSCs: a comparison between meso push-pull and  $\beta$ -pyrrolic architectures. *ACS Appl Mater Interfaces* 2014; 6:15841-52.
- [13] Lindsey JS, Synthetic routes to meso-patterned porphyrins. *Acc Chem Res* 2010; 43:300-11.
- [14] Orbelli Biroli A; Tessore F, Vece V, Di Carlo G, Mussini PR, Trifiletti V, De Marco L, Giannuzzi R, Mancac M, Pizzottib M. Highly improved performance of  $\text{Zn}^{\text{II}}$  tetraarylporphyrinates in DSSCs by the presence of octyloxy chains in the aryl rings. *J Mater Chem A* 2015; 3:2954-9.
- [15] Wang Q, Campbell WM, Bonfantani EE, Jolley KW, Officer DL, Walsh PJ, Gordon K, Humphry-Baker R, Nazeeruddin MK, Grätzel M. Efficient light harvesting by using green Zn-porphyrin-sensitized nanocrystalline  $\text{TiO}_2$  films. *J. Phys. Chem. B* 2005; 109:15397-409.

- [16] Ishida M, Hwang D, Zhang Z, Choi YJ, Oh J, Lynch VM, Kim DY, Sessler JL, Kim D.  $\beta$ -functionalized push-pull porphyrin sensitizers in dye-sensitized solar cells: effect of  $\pi$ -conjugated spacers. *ChemSusChem* 2015; 8:2967-77.
- [17] Chai QP, Li WQ, Wu YZ, Pei K, Liu JC, Geng ZY, Tian H, Zhu WH. Effect of a long alkyl group on cyclopentadithiophene as a conjugated bridge for D-A- $\pi$ -A organic sensitizers: IPCE, electron diffusion length, and charge recombination. *ACS Appl Mater Interfaces* 2014; 6:14621-30.
- [18] Wu YZ, Zhu WH, Zakeeruddin SM, Grätzel M. Insight into D-A- $\pi$ -A structured sensitizers: A promising route to highly efficient and stable dye-sensitized solar cells. *ACS Appl Mater Interfaces* 2015; 7:9307-18.
- [19] Pei K, Wu YZ, Li H, Geng ZY, Tian H, Zhu WH. Cosensitization of D-A- $\pi$ -A quinoxaline organic dye: efficiently filling the absorption valley with high photovoltaic efficiency. *ACS Appl Mater Interfaces* 2015; 7:5296-304.
- [20] Mathew S, Yella A, Gao P, Humphry-Baker R, Curchod BFE, Ashari-Astani N, Tavernelli I, Rothlisberger U, Nazeeruddin MK, Grätzel M. Dye-sensitized solar cells with 13% efficiency achieved through the molecular engineering of porphyrin sensitizers. *Nat Chem* 2014; 6:242-7.
- [21] Lu FT, Wang XX, Zhao YM, Yang G, Zhang J, Zhang B, Feng YQ. Studies on D-A- $\pi$ -A structured porphyrin sensitizers with different additional electron-withdrawing unit. *J Power Sources* 2016; 333:1-9.

- [22] Fan SH, Lv K, Sun H, Zhou G, Wang ZS. The position effect of electron-deficient quinoxaline moiety in porphyrin based sensitizers. *J Power Sources* 2015; 279:36-47.
- [23] Cabau L, Kumar CV, Moncho A, Clifford JN, López N, Palomares E. A single atom change “switches-on” the solar-to-energy conversion efficiency of Zn-porphyrin based dye sensitized solar cells to 10.5%. *Energy Environ Sci* 2015; 8:1368-75.
- [24] Xie YS, Tang YY, Wu WJ, Wang YQ, Liu JC, Li X, Tian H, Zhu WH. Porphyrin cosensitization for a photovoltaic efficiency of 11.5%: A record for non-Ruthenium solar cells based on iodine electrolyte. *J Am Chem Soc* 2015; 137:14055-8.
- [25] Wang CL, Zhang M, Hsiao YH, Tseng CK, Liu CL, Xu MF, Wang P, Lin CY. Porphyrins bearing a consolidated anthryl donor with dual functions for efficient dye-sensitized solar cells. *Energy Environ Sci* 2016; 9:200-6.
- [26] Chang DW, Lee HJ, Kim JH, Park SY, Park SM, Dai LM, Baek JB. Novel quinoxaline-based organic sensitizers for dye-sensitized solar cells. *Org Lett* 2011; 13:3880-3.
- [27] Gao GY, Ruppel JV, Allen DB, Chen Y, Zhang XP. Synthesis of  $\beta$ -functionalized porphyrins via palladium-catalyzed carbon-heteroatom bond

- formations: expedient entry into  $\beta$ -chiral porphyrins. *J Org Chem* 2007; 72:9060-6.
- [28] Zeng Z, Zhang B, Li CJ, Peng X, Liu XJ, Meng SX, Feng YQ. A key point of porphyrin structure affect DSSCs performance based on porphyrin sensitizers. *Dyes Pigm* 2014; 100:278-85.
- [29] Xue XD, Zhang WH, Zhang NN, Ju CG, Peng X, Yang YB, Liang YX, Feng YQ, Zhang B. Effect of the length of the alkyl chains in porphyrin meso-substituents on the performance of dye-sensitized solar cells. *RSC Adv* 2014; 4:8894-900.
- [30] Wu YZ, Zhu WH. Organic sensitizers from D- $\pi$ -A to D-A- $\pi$ -A: effect of the internal electron-withdrawing units on molecular absorption, energy levels and photovoltaic performances. *Chem Soc Rev* 2013; 42:2039-58.
- [31] Kim JJ, Choi H, Lee JW, Kang MS, Song K, Kang SO, Ko J. A polymer gel electrolyte to achieve  $\geq 6\%$  power conversion efficiency with a novel organic dye incorporating a low-band-gap chromophore. *J Mater Chem* 2008; 18:5223-9.
- [32] Hagberg DP, Edvinsson T, Marinado T, Boschloo G, Hagfeldt A, Sun L. A novel organic chromophore for dye-sensitized nanostructured solar cells. *Chem Commun* 2006; 21:2245-7.

- [33] Chou HH, Chen YC, Huang HJ, Lee TH, Lin JT, Tsai C, Chen K. High-performance dye-sensitized solar cells based on 5,6-bis-hexyloxy-benzo[2,1,3]thiadiazole. *J Mater Chem* 2012; 22:10929-38.
- [34] Lenzmann F, Krueger J, Burnside S, Brooks K, Grätzel M, Gal D, Rühle S, Cahen D. Surface photovoltage spectroscopy of dye-sensitized solar cells with TiO<sub>2</sub>, Nb<sub>2</sub>O<sub>5</sub>, and SrTiO<sub>3</sub> nanocrystalline photoanodes: indication for electron injection from higher excited dye states. *J Phys Chem B* 2001; 105:6347-52.
- [35] Cao XW, Lin WY, Yu QX. A ratiometric fluorescent probe for thiols based on a tetrakis (4-hydroxyphenyl)porphyrin coumarin scaffold. *J Org Chem* 2011; 76:7423-30.
- [36] Patel DGD, Feng F, Ohnishi Y, Abboud KA, Hirata S, Schanze KS, Reynolds JR. It takes more than an imine: the role of the central atom on the electron-accepting ability of benzotriazole and benzothiadiazole oligomers. *J Am Chem Soc* 2012; 134:2599-612.
- [37] Yang CH, Chen PY, Chen WJ, Wang TL, Shieh YT. Spectroscopic evidences of synergistic co-sensitization in dye-sensitized solar cells via experimentation of mixture design. *Electrochim Acta* 2013; 107:170-7.
- [38] Yang CH, Lin WC, Wang TL, Shieh YT, Chen WJ, Liao SH, Sun YK. Performance variation from triphenylamine-to

carbazole-triphenylamine-rhodaniline-3-acetic acid dyes in dye-sensitized solar cells. *Mater Chem Phys* 2011; 130:635-43.

[39] Lu FT, Zhang J, Zhou YZ, Zhao YM, Zhang B, Feng YQ. Novel D- $\pi$ -A porphyrin dyes with different alkoxy chains for use in dye-sensitized solar cells. *Dyes Pigm* 2016; 125:116-23.

[40] Thomas KRJ, Kapoor N, Lee CP, Ho KC. Organic dyes containing pyrenylamine-based cascade donor systems with different aromatic  $\pi$  linkers for dye-sensitized solar cells: optical, electrochemical, and device characteristics. *Chem Asian J* 2012; 7:738-50.

**Table 1** Photophysical properties of the three sensitizers

Dye	$\lambda_{\text{abs}}^a$ /nm ( $\epsilon/10^3 \text{ M}^{-1} \text{ cm}^{-1}$ )	Emission $^b$ /nm
<b>LP-4</b>	435(306), 566(22), <b>603</b> (10)	616
<b>LP-5</b>	433(223), 464 (109), 570(27), 605(14)	619
<b>LP-6</b>	431(220), 471(82), 569(26), 606(17)	618

<sup>a</sup> Absorption spectra was measured in THF solution ( $3.0 \times 10^{-6} \text{ M}$ ) at room temperature.

<sup>b</sup> Emission spectra was obtained at 298 K in THF solution by exciting at 420 nm.

**Table 2** Electrochemical data for the porphyrin sensitizers

Dye	$E_{\text{ox}}^a/\text{eV}$	$E_{0-0}^b/\text{eV}$	$E_{\text{HOMO}}^c/\text{eV}$	$E_{\text{LUMO}}^d/\text{eV}$
<b>LP-4</b>	0.35	2.07	-5.15	-3.08
<b>LP-5</b>	0.42	2.05	-5.22	-3.17
<b>LP-6</b>	0.43	2.04	-5.23	-3.19

<sup>a</sup> First oxidation potentials vs ferrocene/ferrocenium (Fc/Fc<sup>+</sup>) couple. <sup>b</sup>  $E_{0-0}$  was determined from the intersection of normalized absorption and emission spectra. <sup>c</sup>

$$E_{\text{HOMO}} = -4.8\text{eV} - E_{\text{ox}} \quad . \quad ^d E_{\text{LUMO}} = E_{\text{HOMO}} - E_{0-0}.$$

**Table 3** Photovoltaic parameters of porphyrin-sensitized solar cells

Dye	dye adsorbed amount <sup>a</sup> (10 <sup>-7</sup> mol cm <sup>-2</sup> )	$J_{sc}$ (mA cm <sup>-2</sup> )	$V_{oc}$ (mV)	$FF$	$\eta$ (%)
<b>LP-4</b>	1.41	7.60	720	0.73	4.02
<b>LP-5</b>	1.66	9.03	660	0.75	4.47
<b>LP-6</b>	1.59	11.47	710	0.74	6.14
<b>N719<sup>b</sup></b>		14.89	780	0.70	8.11

<sup>a</sup> The amount of the dye adsorbed on the TiO<sub>2</sub> surface was estimated spectroscopically by desorbing the dye with a 0.1 M solution of NaOH in anhydrous ethanol. <sup>b</sup> As a reference, the overall efficiency of **N719** sensitized solar cells was determined.

## Figure Captions

**Fig. 1** Molecular structure of the three porphyrin sensitizers

**Fig. 2** UV-visible absorption spectra of compound **LP-4**, **LP-5** and **LP-6** (a) in THF solutions and (b) on transparent TiO<sub>2</sub> films (4  $\mu$ m).

**Fig. 3** Energy levels (eV) of HOMO and LUMO molecular orbitals for the three sensitizers

**Fig. 4** Calculated frontier molecular orbitals for the porphyrin dyes.

**Fig. 5** (a) The J-V curves and (b) the IPCE profiles of **LP-4**, **LP-5** and **LP-6** sensitizers

**Fig. 6** Nyquist plots (a) and Bode-phase plots (b) of electrochemical impedance

**Scheme 1** The synthetic routes for the three dyes

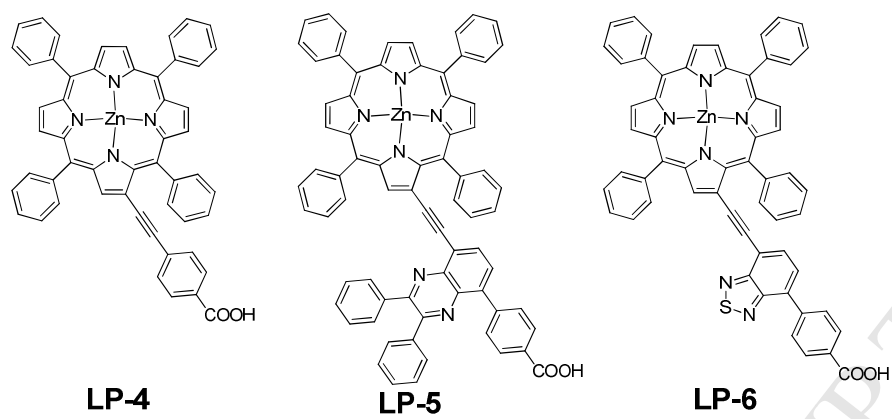


**Fig. 1** Molecular structure of the three porphyrin sensitizers

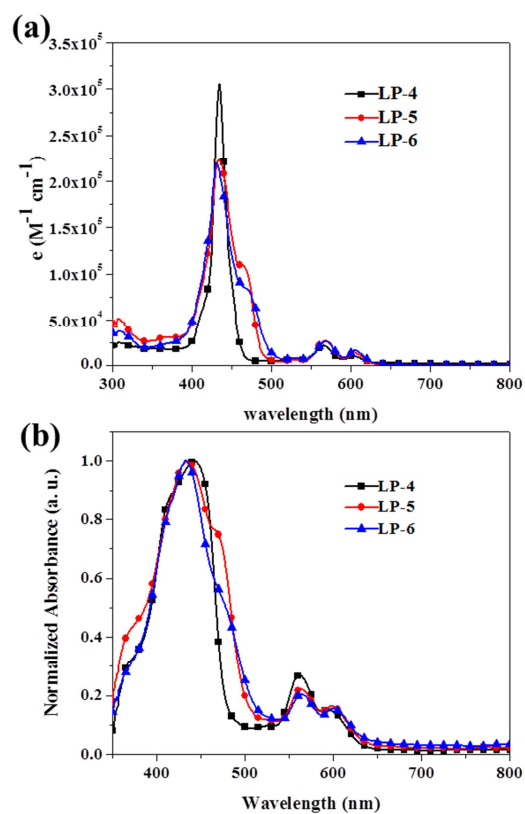


**Fig. 2** UV-visible absorption spectra of compound **LP-4**, **LP-5** and **LP-6** (a) in THF solutions and (b) on transparent  $\text{TiO}_2$  films (4  $\mu\text{m}$ ).

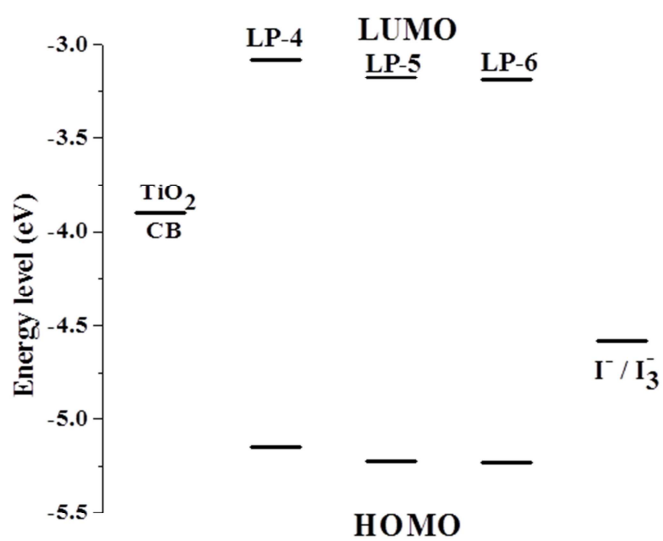


**Fig. 3** Energy levels (eV) of HOMO and LUMO molecular orbitals for the three sensitizers

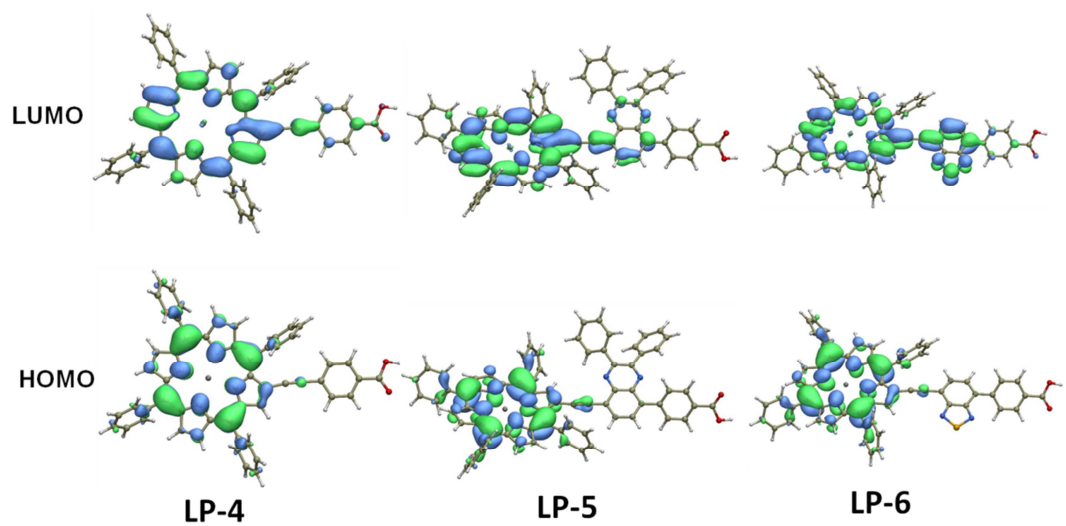


**Fig. 4** Calculated frontier molecular orbitals for the porphyrin dyes.

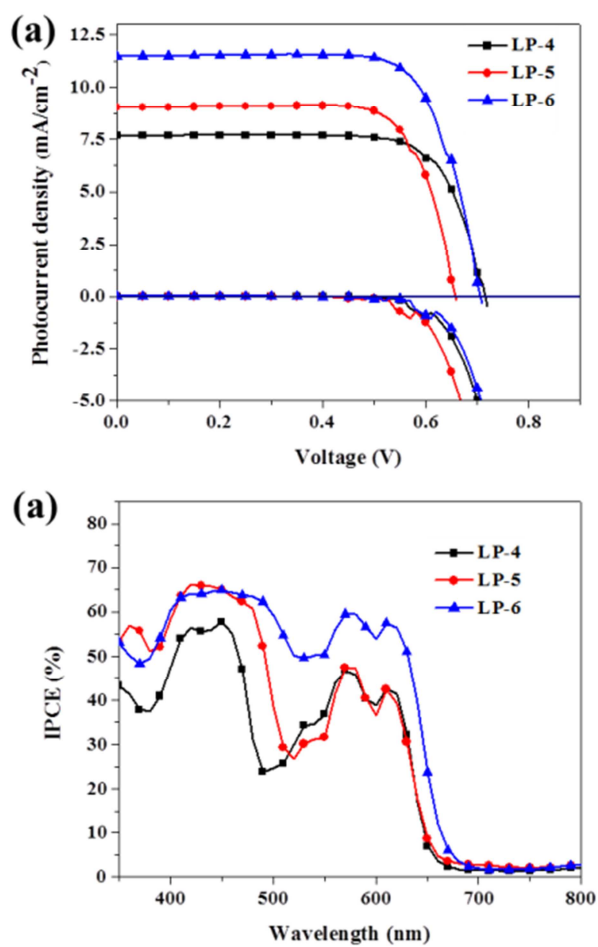


**Fig. 5** (a) The *J-V* curves and (b) the IPCE profiles of LP-4, LP-5 and LP-6 sensitizers

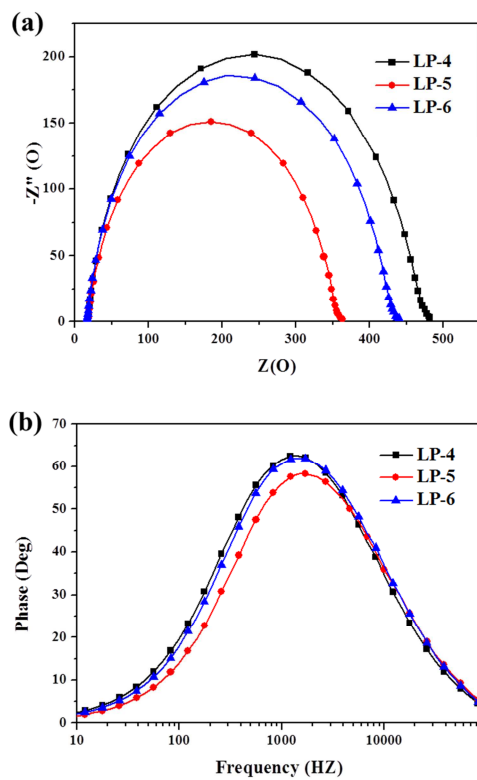


**Fig. 6** Nyquist plots (a) and Bode-phase plots (b) of electrochemical impedance



### Highlight

- Two novel  $\beta$ -functionalized D-A- $\pi$ -A porphyrins are designed and synthesized.
- Introduction of additional acceptors in sensitizers influence the optoelectronic properties.
- A more electron-withdrawing acceptor is optimal for the enhancement of cell efficiency.